Three-Dimensional Probabilistic Foundation Settlement

Gordon A. Fenton, M.ASCE,[1] and D. V. Griffiths, F.ASCE[2]

Abstract: By modeling soil as a three-dimensional spatially random medium, the reliability of shallow foundations against serviceability limit state failure, in the form of excessive settlement and/or differential settlement, can be estimated. The soil's elastic modulus, E, is represented as a lognormally distributed random field with an isotropic correlation structure. The settlements of individual and pairs of square footings placed on the surface of the soil are computed using the finite element method. A probabilistic model for total and differential settlement is presented and compared to results obtained using Monte Carlo simulation. The distributions of total and differential settlement are found to be closely predicted using the distributions of geometric averages of the underlying soil elastic modulus field.

Introduction

Since the design of shallow foundations is most often governed by settlement requirements, a reliability-based approach to their design necessitates knowledge about the distribution of settlement under a given footing. Traditional approaches to the design problem involve estimating the elastic modulus and designing the footing to avoid excessive settlements. Aside from very large total settlements, it is usually differential settlement which leads to serviceability problems. Existing code requirements limiting differential settlements to satisfy serviceability limit states [see building codes ACI 318-89 (ACI 1989) or CAN3-A23.3-M84 (CSA 1984)] specify maximum deflections ranging from $D/180$ to $D/480$, depending on the type of supported elements, where D is the center-to-center span of the supported structural element. In practice, differential settlements between footings are generally controlled, not by considering the differential settlement itself, but by controlling the total settlement predicted by analysis using an estimate of the soil elasticity. This approach is largely based on correlations between total settlements and differential settlements observed experimentally (see, for example, D'Appolonia et al. 1968) and leads to a limitation of 4 to 8 cm in total settlement under a footing as stipulated by the *Canadian Foundation Engineering Manual*, Part 2 (CGS 1978).

This paper presents a study of the probability distributions of settlement and differential settlement where the soil is modeled as a fully three-dimensional random field and footings have both

[1]Professor, Dept. of Engineering Mathematics, Dalhousie Univ., Halifax, NS, B3J 2X4 Canada. E-mail: gordon.fenton@dal.ca

[2]Professor, Division of Engineering, Colorado School of Mines, Golden, CO 80401-1887. E-mail: vgriffit@mines.edu

length and breadth. The study is an extension of previous work by the writers (Fenton and Griffiths 2002), which used a two-dimensional random soil to investigate the behavior of a strip footing of infinite length. The resulting two-dimensional probabilistic model is found to also apply in concept to the three-dimensional case here. Improved results are given for differential settlement by using a bivariate lognormal distribution, rather than the approximate univariate normal distribution used in Fenton and Griffiths (2002).

The paper first considers the case of a single square rigid pad footing, a cross section which is shown in Fig. 1(a), and estimates the probability density function governing the total settlement of the footing as a function of footing area for various statistics of the underlying soil. Only the soil elasticity is considered to be spatially random. Uncertainties arising from model and test procedures and in the loads are not considered. In addition, the soil is assumed to be isotropic—that is, the correlation structure is assumed to be the same in both the horizontal and vertical directions. Although soils generally exhibit a stronger correlation in the horizontal directions, due to their layered nature, the degree of anisotropy is site specific. Considering that, this study is attempting to establish the basic probabilistic behavior of settlement, anisotropy is left as a refinement for site-specific investigations. The writers expect that the averaging model suggested in this paper will drift from a geometric average to a harmonic average as the ratio of horizontal to vertical correlation lengths increases (see also the section entitled, "Single-Footing Case"). Although it is felt that the results of this paper can still be used conservatively by using an effective isotropic correlation length equal to the minimum correlation length, this contention needs testing.

The footings are assumed to be founded on a soil layer underlain by bedrock. The assumption of an underlying bedrock can be relaxed if a suitable averaging region is used—recommendations about such an area are given by Fenton and Griffiths (2002).

The second part of the paper addresses the issue of differential settlements under a pair of footings, as shown in Fig. 1(b), again for the particular case of footings founded on a soil layer underlain by bedrock. The footing spacing is held constant at $D=1$ while varying the footing size. Both footings are square and the same size. The mean and standard deviation of differential settle-
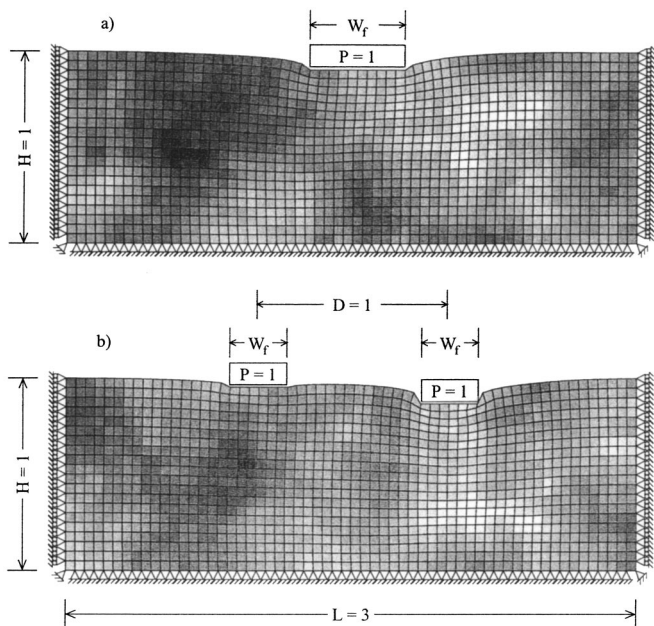
Fig. 1. Slices through a random field/finite element method mesh of: (a) a single footing and (b) two footings founded on a soil layer

ments are estimated as functions of footing size for various input statistics of the underlying elastic modulus field. The probability distribution governing differential settlement is found to be reasonably approximated using a joint lognormal distribution with correlation predicted using local geometric averages of the elastic modulus field under the two footings.

Random Field Finite Element Model

The soil mass is discretized into 60 eight-noded brick elements in each of the horizontal directions by 20 elements in the vertical direction. Each element is cubic with side length 0.05 giving a soil mass which has plan dimension of 3×3 and depth of 1. (Note: Length units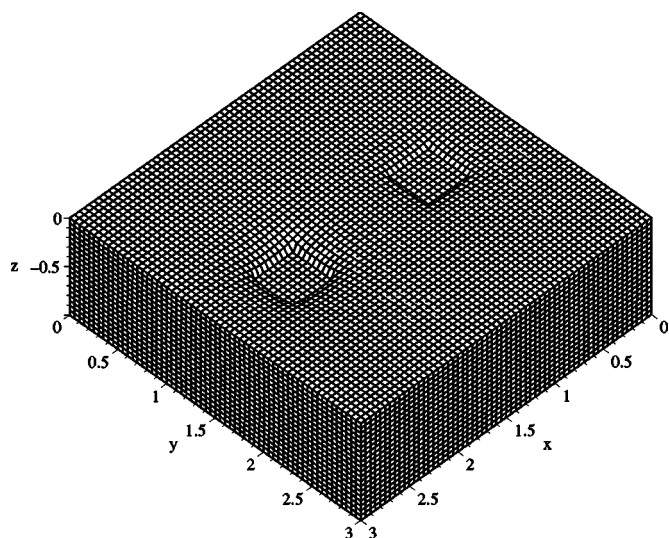 are not used here since the results can be used with any consistent set of length and force units.) Fig. 2 shows the finite element mesh in three dimensions for the case of two footings.

The finite element analysis uses a preconditioned conjugate gradient iterative solver [see, e.g., Smith and Griffiths (1998)] that avoids the need to assemble the global stiffness matrix. Numerical experimentation indicates that the finite element model gives excellent agreement with analytical results for a flexible footing. In the case of a rigid footing, doubling the number of elements in each direction resulted in a settlement which increased by about 3%, indicating that the rigid footing model may be slightly too stiff at the current resolution. However, the stochastic behavior will be unaffected by such slight shifts in total settlement (i.e., by the same fraction for each realization). The 60 by 60 by 20 discretization was considered adequate to characterize the behavior of the settlement and differential settlement probability distributions.

The vertical side faces of the finite element model are constrained against horizontal displacement but are free to slide vertically while the nodes on the bottom boundary are spatially fixed. The footing(s) are assumed to be rigid, to not undergo any rotations, and to have a rough interface with the underlying soil (no-slip boundary). A fixed load $P=1$ is applied to each footing—since settlement varies linearly with load, the results are easily scaled to different values of P.

To investigate the effect of the square footing area, the soil layer thickness, H, was held constant at 1.0, while the footing plan dimension, W_f, was varied according to Table 1. Because the settlement problem is linear in some of its parameters, the following results can be scaled to arbitrary square footing areas as long as the ratio W_f/H is held fixed [note that the latter restriction also holds in the two-dimensional case which was inadvertently not mentioned in Fenton and Griffiths (2002)]. For example, the settlement of a square footing of dimension $W_f=0.2$ m on an $H=1$ m thick soil layer with load $P'=1$ kN and elastic modulus $E=1$ kN/m^2 corresponds to 1.2 times the settlement of a footing of width $W_f'=4.0$ m on an $H'=20.0$ m thick soil layer with $P'=1,000$ kN and elastic modulus $E'=60$ kN/m^2. The scaling factor is $(P/P')(E'/E)(W_f'/W_f)$, as long as $W_f'/H'=W_f/H$.

In the two-footing case, the distance between footing centers was held constant at 1.0, while the footing widths (assumed equal) were varied. Footings of widths greater than 0.8 were not considered since this situation becomes basically that of a strip footing (the footings are joined when $W_f=1.0$). The soil has two properties of interest to the settlement problem: These are the (effective) elastic modulus, $E(\underline{x})$, and Poisson's ratio, $\nu(\underline{x})$, where $\underline{x}$ is spatial position. Only the elastic modulus is considered to be a spatially random soil property. Poisson's ratio was believed to have a smaller relative spatial variability and only a second-order importance to settlement statistics. It is held fixed at 0.25 over the entire soil mass for all simulations.

Fig. 2. Finite element mesh modeling soil supporting two footings

Fig. 1 shows a gray-scale representation of a possible realization of the elastic modulus field along a vertical plane through the soil mass cutting through the footing. Lighter areas denote smaller values of $E(\underline{x})$ so that the elastic modulus field shown in Fig. 1(b) corresponds to a higher elastic modulus under the left footing than under the right—this leads to the substantial differential settlement indicated by the deformed mesh. This is just one possible realization of the elastic modulus field; the next realization could just as easily show the opposite trend.

The elastic modulus field is assumed to follow a lognormal distribution so that $\ln(E)$ is a Gaussian (normal) random field with mean $\mu_{\ln E}$, and variance $\sigma^2_{\ln E}$. The choice of a lognormal distribution is motivated in part by the fact that the elastic modulus is strictly non-negative, a property of the lognormal distribution (but not the normal), while still having a simple relationship with the normal distribution. In addition, soil properties are generally measured as averages over some volume, and these averages are often *low-strength dominated*, as may be expected. The writers have found in this and other studies that the geometric average well represents such low-strength-dominated soil properties. Since the distribution of a geometric average of positive quantities tends to the lognormal distribution by the central limit theorem, the lognormal distribution may very well be a natural distribution for many spatially varying soil properties. The parameters of the transformed $\ln(E)$ Gaussian random field may be obtained from the relations

$$\sigma^2_{\ln E} = \ln(1 + \sigma^2_E/\mu^2_E) \tag{1a}$$

$$\mu_{\ln E} = \ln(\mu_E) - \frac{1}{2}\sigma^2_{\ln E} \tag{1b}$$

from which it can be seen that the log-elastic modulus variance, $\sigma^2_{\ln E}$, varies from 0.01 to 2.83 in this study.

A Markovian spatial correlation function, which gives the correlation coefficient between log-elastic modulus values at points separated by the distance τ, is used

$$\rho_{\ln E}(\underline{\tau}) = \exp\left\{ -\frac{2|\underline{\tau}|}{\theta_{\ln E}} \right\} \tag{2}$$

where $\underline{\tau} = \underline{x} - \underline{x}' =$ vector between spatial points $\underline{x}$ and $\underline{x}'$; and $|\underline{\tau}|$ = absolute length of this vector (the lag distance). In this paper, the word "correlation" refers to the correlation coefficient. The results presented here are not particularly sensitive to the choice in functional form of the correlation—the Markov model is popular because of its simplicity. The correlation function decay rate is governed by the so-called scale of fluctuation, $\theta_{\ln E}$, which, loosely speaking, is the distance over which log-elastic moduli are significantly correlated (when the separation distance $|\underline{\tau}|$ is greater than $\theta_{\ln E}$, the correlation between $\ln E(\underline{x})$ and $\ln E(\underline{x}')$ is less than 14%). The correlation structure is assumed to be isotropic in this study which is appropriate for establishing the basic stochastic behavior of settlement. Anisotropic studies are more appropriate for site-specific analyses.

As was found in the two-dimensional case for the two footing case (e.g., Fenton and Griffiths 2002), using a scale of fluctuation, $\theta_{\ln E}$, equal to the footing spacing, D, is conservative in that it yields the largest probabilities of differential settlement. For total settlement of a single footing, taking $\theta_{\ln E}$ large is conservative since this leads to the largest variability of settlement (least variance reduction due to averaging of the soil properties under the footing).

To investigate the effect of the scale of fluctuation, $\theta_{\ln E}$, on the settlement statistics, $\theta_{\ln E}$ is varied from 0.01 (i.e., very much smaller than the footing and/or footing spacing) to 10.0 (i.e., substantially larger than the footing and/or footing spacing). In the limit as $\theta_{\ln E} \rightarrow 0$, the elastic modulus field becomes a white noise field, with independent E values at any two distinct points. In terms of the finite elements themselves, values of $\theta_{\ln E}$ smaller than the elements result in a set of elements which are largely independent (increasingly independent as $\theta_{\ln E}$ decreases). But because the footing effectively averages the elastic modulus field on which it is founded, and since averages have decreased variance, the settlement in the limiting case $\theta_{\ln E} \rightarrow 0$ is expected to approach that obtained in the deterministic case, with E equal to its median everywhere (assuming geometric averaging), with vanishing variance for finite $\sigma^2_{\ln E}$.

At the other extreme, as $\theta_{\ln E} \rightarrow \infty$, the elastic modulus field becomes the same everywhere. In this case, the settlement statistics are expected to approach those obtained by using a single lognormally distributed random variable, E, to model the soil, $E(\underline{x}) = E$. That is, since the settlement, δ, under a footing founded on a soil layer with uniform (but random) elastic modulus E is given by

$$\delta = \frac{\delta_{\det}\mu_E}{E}, \tag{3}$$

where $\delta_{\det} =$ computed settlement when $E = \mu_E$ everywhere, then, as $\theta_{\ln E} \rightarrow \infty$, the settlement assumes a lognormal distribution with parameters

$$\mu_{\ln \delta} = \ln(\delta_{\det}) + \ln(\mu_E) - \mu_{\ln E} = \ln(\delta_{\det}) + \frac{1}{2}\sigma^2_{\ln E} \tag{4a}$$

$$\sigma_{\ln \delta} = \sigma_{\ln E} \tag{4b}$$

where Eq. (1b) was used in Eq. (4a).

By similar reasoning, the differential settlement between two footings [see Fig. 1(b)] as $\theta_{\ln E} \rightarrow 0$ is expected to go to zero since the average elastic modulus seen by both footings approach the same value, namely the median (assuming geometric averaging). At the other extreme, as $\theta_{\ln E} \rightarrow \infty$, the differential settlement is also expected to approach zero, since the elastic modulus field becomes the same everywhere. Thus, the differential settlement approaches zero at both very small and at very large scales of fluctuation—the largest differential settlements will occur at scales somewhere in between these two extremes. This "worst case" scale has been observed by other researchers—see, for example, the work on a flexible foundation by Baecher and Ingra (1981).

The Monte Carlo approach adopted here involves the simulation of a realization of the elastic modulus field and subsequent finite element analysis (e.g., Smith and Griffiths 1998) of that realization to yield a realization of the footing settlement(s). Repeating the process over an ensemble of realizations generates a set of possible settlements which can be plotted in the form of a histogram and from which distribution parameters can be estimated.

If it can be assumed that log-settlement is approximately normally distributed (which is seen later to be a reasonable assumption and is consistent with the distribution selected for E), and $m_{\ln \delta}$ and $s^2_{\ln \delta}$ are the estimators of the mean and variance of log settlement, respectively, then the standard deviation of these estimators obtained from the $n = 100$ realizations performed for the single footing case are given by
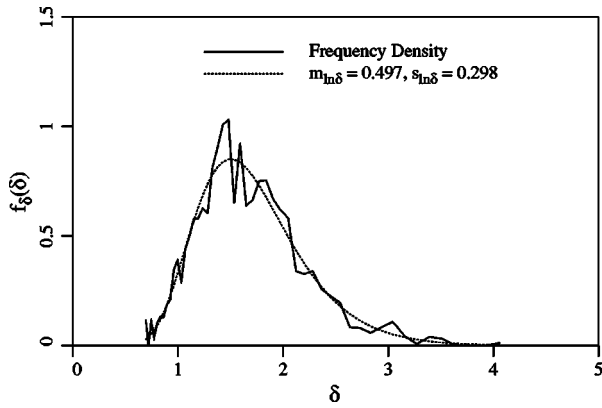
Fig. 3. Typical frequency density plot and fitted lognormal distribution of settlement under a single footing

Fig. 4. Estimated mean of log settlement

$$\sigma_{m_{\ln \delta}} \simeq s_{\ln \delta}/\sqrt{n} = 0.1 s_{\ln \delta} \qquad (5a)$$

$$\sigma_{s^2_{\ln \delta}} \simeq \sqrt{\frac{2}{n-1}} s^2_{\ln \delta} = 0.14 s^2_{\ln \delta} \qquad (5b)$$

These estimator errors are not particularly small but, since the three-dimensional analysis is very time consuming, the number of realizations selected was deemed sufficient to verify that the geometric averaging model suggested in the two-dimensional case is also applicable in three dimensions. A subset of the cases considered in Table 1 (see starred quantities) was rerun using 1,000 realizations to verify the probability distributions further out in the tails for the differential settlement problem.

Realizations of the log-elastic modulus field are produced using the three-dimensional Local Average Subdivision (LAS) technique (Fenton and Vanmarcke 1990; Fenton 1994). The elastic modulus value assigned to the ith element is

$$E(\underline{x}_i) = \exp\{\mu_{\ln E} + \sigma_{\ln E} G(\underline{x}_i)\} \qquad (6)$$

where $G(\underline{x}_i)$=local average, over the element centered at $\underline{x}_i$, of a zero mean unit variance Gaussian random field.

Single-Footing Case

A typical histogram of the settlement under a single footing is shown in Fig. 3 for W_f=0.4, σ_E/μ_E=0.5, and $\theta_{\ln E}$=1.0 (1,000 realizations were performed for this case to increase the resolution of the histogram). With the requirement that settlement be non-negative, the shape of the histogram suggests a lognormal distribution, which was adopted in this study [see, also, Eq. (4a)]. The histogram is normalized to produce a frequency density plot, where a straight line is drawn between the interval midpoints. A Chi-square goodness-of-fit test on the data of Fig. 3 yielded a p value of 0.54 indicating very good support for the lognormal hypothesis. The fitted lognormal distribution, with parameters given by $m_{\ln \delta}$ and $s_{\ln \delta}$ shown in the line key, is superimposed on the plot.

Accepting the lognormal distribution as a reasonable fit to the simulation results, the next task is to estimate the parameters of the fitted lognormal distributions as functions of the input parameters (W_f, σ_E, and $\theta_{\ln E}$). The lognormal distribution
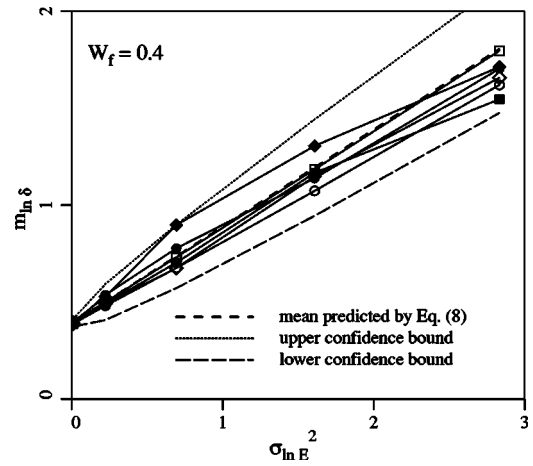
$$f_\delta(x) = \frac{1}{\sqrt{2\pi}\sigma_{\ln \delta} x} \exp\left\{-\frac{1}{2}\left(\frac{\ln x - \mu_{\ln \delta}}{\sigma_{\ln \delta}}\right)^2\right\}, \quad 0 \le x < \infty \quad (7)$$

has two parameters, $\mu_{\ln \delta}$ and $\sigma_{\ln \delta}$. Fig. 4 shows how the estimator of $\mu_{\ln \delta}$, $m_{\ln \delta}$, varies with $\sigma_{\ln E}$ for W_f=0.4 based on 100 realizations. All scales of fluctuation are drawn in the plot, but are not individually labeled since they lie so close together. Also shown in the plot are the 95% confidence interval bounds on the true parameter, $\mu_{\ln \delta}$. As can be seen, all the estimators lie within these bounds indicating that the three-dimensional results are much the same as found using a two-dimensional model, namely that $\mu_{\ln \delta}$ is well predicted by the equation [see Eq. (4a)],

$$\mu_{\ln \delta} = \ln(\delta_{\text{det}}) + \frac{1}{2}\sigma^2_{\ln E} \qquad (8)$$

where δ_{det} is the "deterministic" settlement obtained from a single finite element analysis (or appropriate approximate calculation) of the problem using $E=\mu_E$ everywhere. This equation is also shown in Fig. 4, and it can be seen that the agreement with estimated values of $\mu_{\ln \delta}$ is very good. The other footing sizes considered showed similar results.

Estimates of the standard deviation of log settlement, $s_{\ln \delta}$, are plotted in Fig. 5 (as symbols) for two footing sizes based on 100 realizations. The other footing sizes gave similar results. In all cases, $s_{\ln \delta}$ increases to $\sigma_{\ln E}$ as $\theta_{\ln E}$ increases, which is as expected since large scales give less variance reduction. Assuming that local geometric averaging of the volume directly under the footing accounts for all of the variance reduction seen in Fig. 5, the standard deviation of log settlement is predicted by

$$\sigma_{\ln \delta} = \sqrt{\gamma(W_f, W_f, H)}\sigma_{\ln E} \qquad (9)$$

where $\gamma(W_f, W_f, H)$=so-called variance function (Vanmarcke 1984), giving the amount that the variance is reduced due to averaging. It depends on the averaging volume, $W_f \times W_f \times H$ as well as on the scale of fluctuation, $\theta_{\ln E}$. The agreement between Eq. (9) and the estimated standard deviations is remarkable, as shown in Fig. 5, indicating that a geometric average of the elastic modulus field under the footing is a good model of the effective modulus seen by the footing. The geometric average, E_g, has the following mathematical definition (for a square footing)
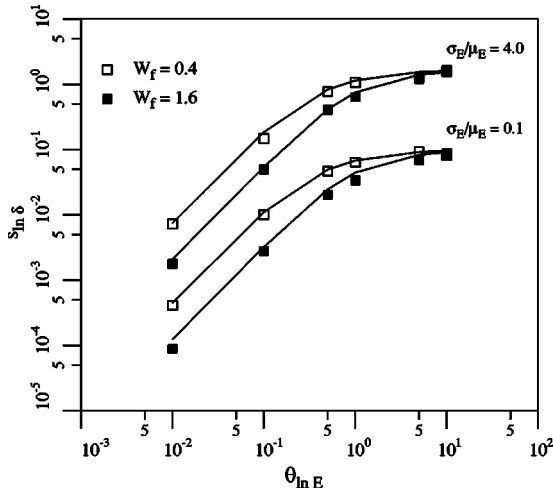
Fig. 5. Comparison of simulated sample standard deviation of log-settlement shown with symbols, with theoretical estimate via Eq. (9) shown with lines

$$E_g = \exp\left(\frac{1}{W_f^2 H}\int_0^H \int_0^{W_f} \int_0^{W_f} \ln E(x,y,z)dx\,dy\,dz\right) \quad (10)$$

from which the settlement of the footing can be expressed as

$$\delta = \frac{\delta_{\text{det}}\mu_E}{E_g} \quad (11)$$

Taking the logarithm of Eq. (11), and expectations, leads to Eqs. (8) and (9). The practical implication of this result is that settlements are better predicted using an effective elastic modulus computed as a geometric average of the experimentally obtained moduli under the footing. For example, if n observations of the elastic modulus under a footing are taken, $E_1, E_2, \ldots, E_n$, then the footing settlement is best computed using the elastic modulus E_g computed as

$$E_g = \left(\prod_{i=1}^n E_i\right)^{1/n} = \exp\left(\frac{1}{n}\sum_{i=1}^n \ln E_i\right) \quad (12)$$

To lend support to the geometric average idea, consider the settlement of a horizontally layered soil, where the elastic modulus varies only from layer to layer but is constant within each layer. It is relatively simple to show that the effective elastic modulus seen by a footing in this case is the harmonic average, if edge effects are ignored

$$E_h = \left[\frac{1}{H}\int_0^H \frac{dz}{E(z)}\right]^{-1} \quad (13)$$

where H=soil depth. Alternatively, if the layers are oriented vertically, the effective elastic modulus seen by a rigid footing becomes the arithmetic average of the layer moduli. The true situation will lie somewhere between these two extremes. Since the geometric average of a random field lies between the arithmetic and harmonic averages, its use in the more general case appears reasonable. Note, however, that this argument suggests that a harmonic average would be more reasonable for a strongly layered soil, a situation which is not considered in this study.

Once the parameters of the settlement distribution, $\mu_{\ln\delta}$ and $\sigma_{\ln\delta}$, have been calculated using Eqs. (8) and (9), probabilities associated with settlement are easily found

$$P[\delta \le x] = \Phi\left(\frac{\ln x - \mu_{\ln\delta}}{\sigma_{\ln\delta}}\right) \quad (14)$$

where Φ=cumulative standard normal function.

Two-Footing Case

Consider now the case of two square footings each of plan dimension $W_f \times W_f$ and separated by center-to-center distance $D = 1$, as shown in Fig. 1(b). If the settlements, δ_1 and δ_2, under each footing are lognormally distributed, as found in the previous section, then the joint distribution between the two-footing settlements follows a bivariate lognormal distribution [Fenton and Griffiths (2002), corrected to include the omitted factor of 2 on the correlation term]

$$f_{\delta_1\delta_2}(x,y) = \frac{1}{2\pi\sigma_{\ln\delta}^2 rxy}\exp\left\{-\frac{1}{2r^2}[\Psi_1^2 - 2\rho_{\ln\delta}\Psi_1\Psi_2 + \Psi_2^2]\right\},$$
$$x \ge 0, \ y \ge 0 \quad (15)$$

where $\Psi_1 = (\ln x - \mu_{\ln\delta})/\sigma_{\ln\delta}$; $\Psi_2 = (\ln y - \mu_{\ln\delta})/\sigma_{\ln\delta}$; $r^2 = 1 - \rho_{\ln\delta}^2$; and $\rho_{\ln\delta}$=correlation coefficient between the log settlement of the two footings. It is assumed in the above that δ_1 and δ_2 have the same mean and variance, which, for the symmetric conditions shown in Fig. 1(b), is a reasonable assumption.

Defining the differential settlement between footings to be $\Delta = \delta_1 - \delta_2$, then the mean of Δ is zero if the elastic modulus field is statistically stationary, as assumed here (if not, then the differential settlement due to any trend in the mean must be handled separately). If Eq. (15) holds, then the exact distribution governing the differential settlement is given by

$$f_\Delta(x) = \int_0^\infty f_{\delta_1\delta_2}(|x| + y, y)dy \quad (16)$$

and differential settlement probabilities can be computed as

$$P[|\Delta| > x] = P[\Delta < -x \cup \Delta > x] = 2\int_x^\infty f_\Delta(\xi)d\xi \quad (17)$$

Fig. 6 shows typical frequency–density plots of differential settlement, for three different values of $\theta_{\ln E}$, between two equal sized footings with $W_f = 0.4$ and $\sigma_E/\mu_E = 1.0$. For small scales of fluctuation, the density plot looks reasonably normal, but for larger scales of fluctuation, the density has a sharper mode with longer tails. Notice that the widest distribution occurs when $\theta_{\ln E}/D$ is equal to about 1.0, indicating that this is a worst case when it comes to differential settlement.

The distribution $f_{\delta_1\delta_2}$, and thus also f_Δ, has three parameters, $\mu_{\ln\delta}$, $\sigma_{\ln\delta}$, and $\rho_{\ln\delta}$. The mean and standard deviation can be estimated using Eqs. (8) and (9) from the previous section. Since local averaging of the log-elastic modulus field under the footing was found to be an accurate predictor of the variance of log settlement, it is reasonable to suggest that the covariance between log settlements under a pair of footings will be well predicted by the covariance between local averages of the log-elastic modulus field under each footing. For equal sized footings, the covariance between local averages of the log-elastic modulus field under two footings separated by distance D is given by
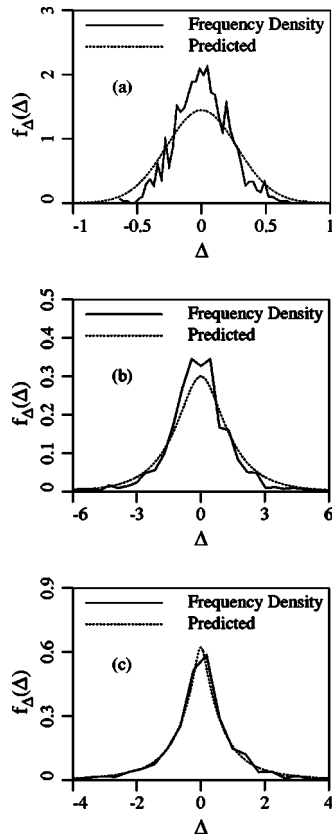
Fig. 6. Frequency density and fitted distribution for differential settlement under two equal-sized footings with $\theta_{\ln E}/D=0.1$ in (a); $\theta_{\ln E}/D=1.0$ in (b); and $\theta_{\ln E}/D=10.0$ in (c)

$$C_{\ln \delta} = \frac{\sigma_{\ln E}^2}{V_1 V_2} \int_{V_1} \int_{V_2} \rho_{\ln E}(\underline{x}_1 - \underline{x}_2) d\underline{x}_2 d\underline{x}_1 \qquad (18)$$

where $V_1 = W_f \times W_f \times H$ volume under Footing 1; $V_2 =$ equivalent volume under Footing 2; and $\underline{x} =$ spatial position. From this, the correlation coefficient can be computed as

$$\rho_{\ln \delta} = \frac{C_{\ln \delta}}{\sigma_{\ln \delta}^2} \qquad (19)$$

The predicted correlation can be compared to the simulation results by first transforming back from log space

$$\rho_\delta = \frac{\exp\{C_{\ln \delta}\} - 1}{\exp\{\sigma_{\ln \delta}^2\} - 1} \qquad (20)$$

where $\sigma_{\ln \delta}$ is given by Eq. (9). The agreement between the correlation coefficient predicted by Eq. (20) and the correlation coefficient estimated from the simulations (1,000 realizations) is shown in Fig. 7. The agreement is reasonable, particularly for the smaller sized footings. For larger footings, the correlation is underpredicted, particularly at small $\theta_{\ln E}$. This is believed to be due to mechanical interaction between the larger footings, where the settlement of one footing induces some settlement in the adjacent footing due to their relatively close proximity.

Armed with the relationships (8), (9), and (19), the differential settlement distribution, f_Δ, can be computed using Eq. (16). The resulting predicted distributions have been superimposed on the frequency–density plots of Fig. 6 for $W_f=0.4$. The agreement is very good for intermediate to large scales of fluctuation. At the
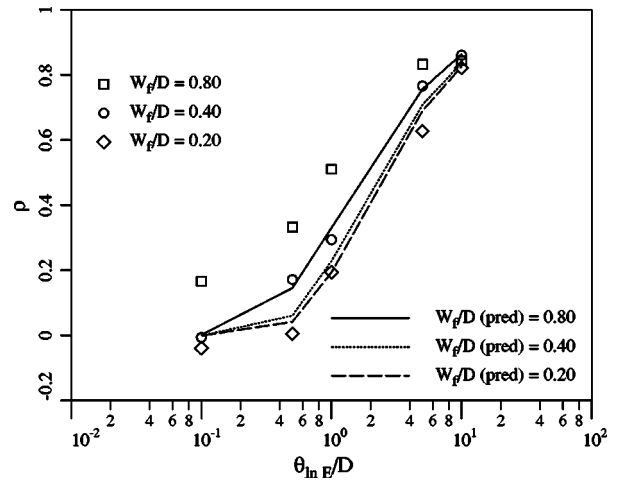

Fig. 7. Predicted and sample correlation coefficients between footing settlements for various relative separation distances between the footings and for $\sigma_E/\mu_E=1$

smaller scales of fluctuation, Eq. (16) yields a distribution which is somewhat too wide—this is due to the underprediction of the correlation between footing settlements [Eq. (19)] since as the actual correlation between settlements increases, the differential settlement decreases and the distribution becomes narrower. However, an underprediction of correlation is at least conservative in that predicted differential settlement probabilities will tend to be too large.

To test the ability of the bivariate lognormal distribution to accurately estimate probabilities, the probability that the absolute value of Δ exceeds some threshold is compared to empirical probabilities derived from simulation. For generality, thresholds of $\alpha\mu_{|\Delta|}$ will be used, where $\mu_{|\Delta|}$ is the mean absolute differential settlement, which can be approximated as (which holds for Δ normally distributed)

$$\mu_{|\Delta|} \simeq \sqrt{\frac{2}{\pi}} \sigma_\Delta \qquad (21)$$

where $\sigma_\Delta^2 = 2\sigma_\delta^2(1-\rho_\delta)$. Fig. 8 shows a plot of the predicted [Eq. (17)] versus empirical probabilities $P[|\Delta|>\alpha\mu_{|\Delta|}]$ for α varying in 20 steps from 0.2 to 4.0. If the prediction is accurate, then the plotted points should lie on the diagonal line.

When the footings are well separated [$W_f/D=0.2$, see Fig. 8(a)] so that mechanical correlation is negligible, then the agreement between predicted and empirical probabilities is excellent. The two solid curved lines shown in the plot form a 95% confidence interval on the empirical probabilities, and it can be seen that most lie within these bounds. The few that lie outside are on the conservative side (predicted probability exceeds empirical probability).

As the footing size increases [see Figs. 8(b and c)] so that their relative spacing decreases, the effect of mechanical correlation begins to be increasingly important and the resulting predicted probabilities increasingly conservative. A strictly empirical correction can be made to the correlation to account for the missing mechanical influences. If $\rho_{\ln \delta}$ is replaced by $(1-W_f/2D)\rho_{\ln \delta} + W_f/2D$ for all W_f/D greater than about 0.3, the differential settlements are reduced and, as shown in Fig. 9, the predicted probabilities become reasonably close to the empirical probabilities while still remaining slightly conservative. Until the complex
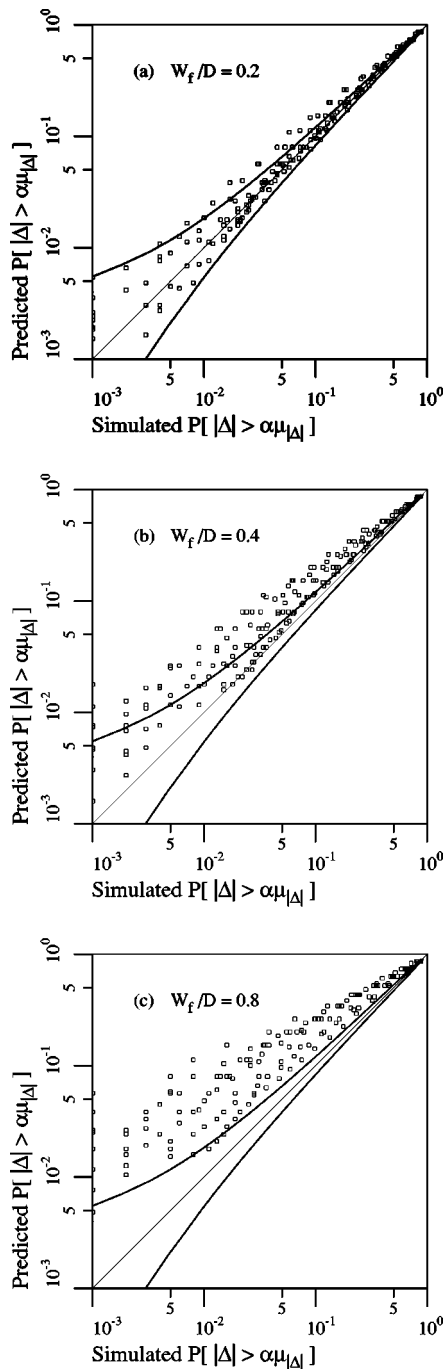
Fig. 8. Predicted versus empirical probabilities $P[|\Delta| > \alpha\mu_{|\Delta|}]$, for $\sigma_E/\mu_E = 0.1$ and 1.0, $\theta_{\ln E}$ varying from 0.1 to 10.0, and for $W_f/D = 0.2$ in (a); $W_f/D = 0.4$ in (b); and $W_f/D = 0.8$ in (c). Curved lines are 95% confidence intervals.

Fig. 9. Predicted versus empirical probabilities $P[|\Delta| > \alpha\mu_{|\Delta|}]$, corrected by empirically increasing $\rho_{\ln \delta}$ for $W_f/D = 0.4$ in (a) and $W_f/D = 0.8$ in (b)

interaction between two relatively closely spaced footings is fully characterized probabilistically, this simple empirical correction seems reasonable.

Conclusions

On the basis of this simulation study, the following observations can be made.

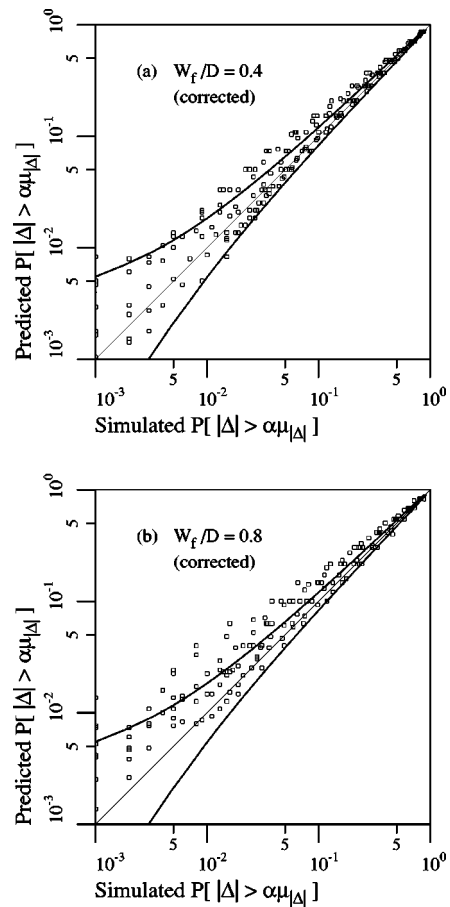As found in the two-dimensional case, the settlement under a footing founded on a three-dimensional spatially random elastic modulus field of finite depth overlying bedrock is well represented by a lognormal distribution with parameters $\mu_{\ln \delta}$ and $\sigma^2_{\ln \delta}$, if E is also lognormally distributed. The first parameter, $\mu_{\ln \delta}$, is dependent on the mean and variance of the underlying log-elastic modulus field and may be closely approximated by considering limiting values of $\theta_{\ln E}$. The second parameter, $\sigma^2_{\ln \delta}$, is very well represented by the variance of a local average of the log-elastic modulus field in the region directly under the footing. Once the parameters of the settlement, $\mu_{\ln \delta}$ and $\sigma^2_{\ln \delta}$, have been computed, using Eqs. (8) and (9), the estimation of probabilities associated with settlement involves little more than referring to a standard normal distribution table [see Eq. (14)].

One of the implications of the findings for a single footing is that footing settlement is accurately predicted using a geometric average of the elastic modulus field in the volume under the footing. From a practical point of view, this finding implies that a geometric average of soil elastic modulus estimates made in the vicinity of the footing (e.g. by cone penetration test soundings) should be used to represent the effective elastic modulus rather than an arithmetic average. The geometric average will generally be less than the arithmetic average, reflecting the stronger influence of weak soil zones on the total settlement.

Under the model of a lognormal distribution for the settlement of an individual footing, the bivariate lognormal distribution was found to closely represent the joint settlement of two footings when the footings are spaced sufficiently far (relative to their plan

dimension) apart to avoid significant mechanical interaction. Using the bivariate lognormal model, probabilities associated with differential settlement are obtained that are in very good agreement with empirical probabilities obtained via simulation. The bivariate lognormal model is considerably superior to the approximate normal model developed in the two-dimensional case by Fenton and Griffiths (2002) at the expense of a more complicated numerical integration (the normal approximation simply involved a table lookup).

When the footings become close enough that mechanical interaction becomes significant, the bivariate lognormal model developed here begins to overestimate the probabilities associated with differential settlement—that is, the differential settlements will be less than predicted. Although this is at least conservative, the reason is believed to be due to the fact that the stress field from one footing is affecting the elastic modulus field under the other footing. This results in an increased correlation coefficient between the two-footing settlements that is not fully accounted for by the correlation between two local geometric averages alone. An empirical correction factor has been suggested in this paper which yields more accurate probabilities and which should be employed if the conservatism without it is unacceptable.

Acknowledgments

Notation

The following symbols are used in this paper:

$C_{\ln \delta}$ = covariance between log settlements under the two footings;
D = center-to-center distance between footings;
E = elastic modulus;
E_g = elastic modulus geometric mean;
f_δ = settlement probability density function;
$f_{\delta_1 \delta_2}$ = joint settlement probability density function;
f_Δ = differential settlement probability density function;
$G(\underline{x})$ = standard normal (Gaussian) random field;
H = overall depth of soil layer;
L = overall width of soil model;
m_δ = estimated mean of footing settlement via simulation;
$m_{\ln \delta}$ = estimated mean of log settlement via simulation;
P = applied footing load;

$s_{\ln \delta}$ = estimated standard deviation of log settlement via simulation;
W_f = footing width;
$\underline{x}$ = spatial coordinate or position;
γ = variance function (variance reduction due to local averaging);
Δ = differential settlement between footings;
δ = footing settlement, positive downward;
δ_{det} = footing settlement when $E = \mu_E$ everywhere;
$\theta_{\ln E}$ = isotropic scale of fluctuation of the log-elastic modulus field;
μ_E = mean elastic modulus;
$\mu_{|\Delta|}$ = mean absolute differential footing settlement;
$\mu_{\ln E}$ = mean of log-elastic modulus;
$\mu_{\ln \delta}$ = mean of log-settlement;
ν = Poisson's ratio;
ρ_δ = correlation coefficient between footing settlements;
$\rho_{\ln \delta}$ = correlation coefficient between log-footing settlements;
$\rho_{\ln E}$ = correlation coefficient between $\ln(E)$ at two points;
σ_E = standard deviation of elastic modulus;
$\sigma_{\ln E}$ = standard deviation of log-elastic modulus;
σ_δ = standard deviation of footing settlement;
$\sigma_{\ln \delta}$ = standard deviation of log-settlement;
σ_Δ = standard deviation of differential settlement;
τ = lag distance, equal to $|\underline{\tau}|$;
$\underline{\tau}$ = spatial lag vector; and
Φ = standard normal cumulative distribution function.

References

American Concrete Institute (ACI). (1989). "Building code requirements for reinforced concrete." *ACI 318-89*, ACI, Detroit.

Baecher, G. B., and Ingra, T. S. (1981). "Stochastic FEM in settlement predictions," *J. Geotech. Eng. Div., Am. Soc. Civ. Eng.*, 107(4), 449–463.

Canadian Geotechnical Society (CGS). (1978). *Canadian foundation engineering manual*, CGS, Montreal, Quebec.

Canadian Standards Association (CSA). (1984). "Design of concrete structures for buildings." *CAN3-A23.3-M84*, CSA, Toronto, Ontario.

D'Appolonia, D. J., D'Appolonia, E., and Brissette, R. F. (1968). "Settlement of spread footings on sand." *J. Soil Mech. Found. Div.*, 94(SM3), 735–760.

Fenton, G. A., and Vanmarcke, E. H. (1990). "Simulation of random fields via local average subdivision." *J. Eng. Mech.*, 116(8), 1733–1749.

Fenton, G. A., and Griffiths, D. V. (2002). "Probabilistic foundation settlement on spatially random soil." *J. Geotech. Geoenviron. Eng.*, 128(5), 381–390.

Fenton, G. A. (1994). "Error evaluation of three random field generators." *J. Eng. Mech.*, 120(12), 2478–2497.

Smith, I. M., and Griffiths, D. V. (1998). *Programming the finite element method*, 3rd Ed., Wiley, New York.

Vanmarcke, E. H. (1984). *Random fields: Analysis and synthesis*, The MIT Press, Cambridge, Mass.